JOURNAL OF MATERIALS SCIENCE 26 (1991) 2057–2062

Correlation of the acoustic emission and the fracture toughness of ductile nodular cast iron

S. H. CARPENTER, ZUMING ZHU*
Physics Department, University of Denver, Denver, CO 80208, USA

Salzbrenner has recently determined the fracture toughness of a series of ductile cast iron samples which were heat treated to produce a fully ferritic matrix. His results indicated that the fracture toughness is strongly dependent upon the average spacing between (or equally the diameter of) the spherical graphite nodules in the ferrite matrix. The acoustic emission generated during the uniaxial compressive deformation of nodular cast iron also depends strongly on the average diameter of the graphite nodules in the test sample. The present investigation was carried out to determine the correlations, if any, between the fracture toughness and the acoustic emission generated during compression of ductile cast iron. The acoustic emission generated during compression was determined using sample materials identical to those used by Salzbrenner. Excellent correlations between certain features of the measured acoustic emission and the fracture toughness were obtained. Data indicate that it should be possible to determine both the fracture toughness and the average size of the graphite nodules from the acoustic emission and load curve generated during a compression test of ductile cast iron.

1. Introduction

In recent years there has been an increased interest in the use of ductile cast iron for a variety of practical applications [1]. Many of the applications reported, i.e. turbine castings, automotive components, transportation and storage casks for radioactive materials, etc., require the enhanced ductility due to the spherical graphite nodules. Proper design requires a working knowledge of the fracture toughness. Previous investigations have shown a wide variation in the fracture toughness of ductile cast iron, with the presence or absence of carbide in a pearlitic morphology reported to be the dominant controlling feature [2–4]. Previously reported work indicates that pearlite in amounts of 15% or greater will cause the ductile cast iron to behave in a linear elastic manner. If 10% or less pearlite is present, however, the ductile cast iron alloys will, in general, behave in an elastic–plastic manner. For those alloys with small amounts of pearlite, elastic–plastic techniques, such as ASTM E-813, must be used to determine the fracture toughness.

Salzbrenner has recently carried out a study of the fracture toughness of a number of ductile cast iron materials which were heat treated to produce a fully ferritic matrix [5]. Heat treatments were carried out to produce samples having different average graphite nodule diameters with little if any pearlite in the matrix. The fracture toughness was determined by the procedures outlined in ASTM E-813. The results obtained showed that the fracture toughness was strongly dependent upon the spacing between (or equally the diameter of) the spherical graphite nodules. As would be expected, the fracture toughness was found to be determined by the ligament distance between the nodules.

Acoustic emission is a transient elastic wave generated by the rapid release of energy within a material. A wide variety of source mechanisms have been proposed and investigated as sources of acoustic emission [6]. Mechanisms have included crack propagation, twin formation, martensitic phase transformations, dislocation avalanche motion and/or multiplication and the fracture and/or debonding of second-phase particles or precipitates. Most materials will produce acoustic emission when plastically deformed. Uniaxial compression of ductile cast iron generates significant acoustic emission [7]. Portions of the acoustic emission (i.e. the acoustic emission generated in a particular portion of the stress–strain curve) from the compression of ductile cast iron are strongly dependent upon the average size of the nodule diameter [7–9]. Experimental data show that the larger the graphite nodules, the more emission is generated.

The purpose of the investigation reported on in this paper was to determine the correlations, if any, between the acoustic emission generated during compressive deformation and the fracture toughness of nodular cast iron. If a strong correlation does exist it may be possible to establish the fracture toughness from monitoring a simple compression test rather than carrying out the more difficult elastic–plastic fracture toughness tests. Possibly the acoustic emis-

* *Permanent address*: Institute of Metals Research, Wehua Road, Shenyang, People's Republic of China.

0022–2461/91 $03.00 + .12

sion measurements will also provide useful and fundamental information and insights into the mechanisms which determine and control the fracture toughness.

2. Experimental Procedure

A series of well-characterized ductile cast iron samples were supplied by Dr R. Salzbrenner, Sandia Laboratories, Albuquerque, NM, for use in the present investigation. The materials supplied were basically the two halves of previously tested compact tension specimens. Compression test specimens were machined from the material supplied as shown schematically in Fig. 1. The dimensions of the compression samples were 7 mm × 10 mm × 20 mm. Before testing, the compression samples were annealed at 700 °C for 24 h and then furnace cooled. The heat treatment was primarily to allow for the relaxation of any residual stresses which might have been introduced during previous testing. Compression tests were carried out at a constant crosshead speed of 0.0064 cm min^{-1} using an MTS-880 deformation machine. The composition and average three-dimensional nodule diameter as determined by Salzbrenner are given in Table I. The microstructure is characterized by nearly spherical graphite nodules in a ferrite matrix. Fig. 2 shows a micrograph of the microstructure for a 7L sample, i.e. an average nodule diameter of 0.031 mm.

The acoustic emission generated during compressive deformation was measured using standard commercial equipment. The transducer used was a resonant type piezoelectric (PZT-5) transducer with a resonant frequency of approximately 140 kHz. Measurements were made at a gain of 105 dB and a bandpass of 100–300 kHz. The amplified RMS voltage from the transducer was measured using a Hewlett–Packard 3400A voltmeter. All RMS voltage data were corrected for the noise level and gain factors and are referenced to the output voltage of the transducer. Care was exercised to eliminate any and all sources of extraneous noise during testing.

3. Results

Previous investigations have reported the generation of significant acoustic emission during the compressive deformation of ductile cast iron [7, 8]. The results presented in this paper are in agreement with previously published data. An example of the acoustic emission generated during the compressive deformation of nodular cast iron is shown in Fig. 3. Fig. 3 is a reproduction of actual strip chart acoustic emission data (in terms of the RMS voltage) and the applied load as a function of crosshead displacement for a ductile cast iron sample from the 4L sample group. An examination of the acoustic emission data reveals the existence of two distinct maxima. The first maximum occurs near yield and is believed to be due to the avalanche motion of dislocations at yield. A peak in the acoustic emission at yield during uniaxial deformation is common behaviour for many materials [10, 11]. The acoustic emission at yield is most often associated with avalanche motion of dislocations and will not be discussed further in this paper. The acoustic emission at strains well past yield forms a broad maxima. The source of this acoustic emission is believed to be the fracture and/or debonding of the graphite nodules in the ferrite matrix [7, 8]. If the source of this acoustic emission is indeed the fracture of the graphite nodules, its magnitude should be dependent on the average size of the graphite nodules. The 4L sample group (Fig. 2) has an average nodule diameter of 0.088 mm. By comparison, Fig. 4 shows the acoustic emission and applied load strip chart data as a function of crosshead displacement for the compressive loading of a sample from the 2U sample group. Samples from the 2U group have an average nodule diameter of 0.123 mm. An examination of the data in the two figures (3 and 4) shows that the magnitude of the acoustic emission is considerably larger in Fig. 4. Table II gives the average numerical values for the pertinent data generated during the acoustic emission measurements along with the average three-dimensional nodule diameter for the different sample groups tested. The column RMS 2nd maximum is a best estimate of the average value of the RMS voltage at its maximum value past yield. A better estimate of the maximum value of the RMS can be obtained from strip charts operated at different speeds and sensitivities from those shown in Figs 3 and 4. The column, "RMS 2nd maximum less back." is the average of the RMS bursts near the 2nd maximum less the value of the background or continuous emission at that point. Analysis of the load deflection curve reveals that the value of the load (applied stress) at the point where the maximum in RMS voltage occurs increases as the average nodule diameter decreases. The values of the applied stress at the 2nd RMS maximum are also given in Table II. As stated earlier, all of the RMS voltage data were corrected for electronic noise and gain and are referenced to the output voltage of the transducer. Data presented in Table II are the averages of four separate tests in each sample group.

A comparison of the experimental data given in Table II with the nodule diameter reveals definite correlations. Basically, the larger the average nodule diameter, the larger the second RMS maximum and the smaller the value of the applied stress at the second RMS maximum. As will be discussed in detail in the next section, the correlations are in fundamental

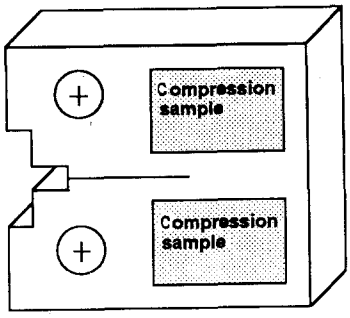

Figure 1 Schematic diagram showing the location of compressive test specimens. Specimens were machined from previously tested fracture toughness specimens.

TABLE I Composition (wt %) and average nodule diameter of the ductile cast iron samples used in the present investigation

Sample group no.	C	Si	Ni	S	Cu	Cr	Mn	Nodule diameter (mm)
5U	2.97	1.70	0.76	0.024	0.083	0.08	0.24	0.136
2U	2.82	1.64	0.66	0.018	0.085	0.08	0.25	0.123
1L	2.88	1.11	0.96	0.022	0.21	0.14	0.26	0.078
4L	3.06	1.16	1.42	0.022	0.21	0.14	0.23	0.088
7L	2.93	2.10	0.79	0.010	0.20	0.14	0.26	0.031

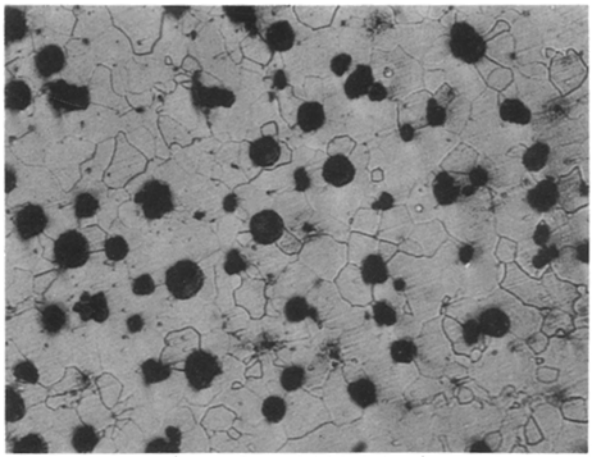

Figure 2 Micrograph of a sample from the 7L group at a magnification of × 183. The average nodule diameter is 0.031 mm.

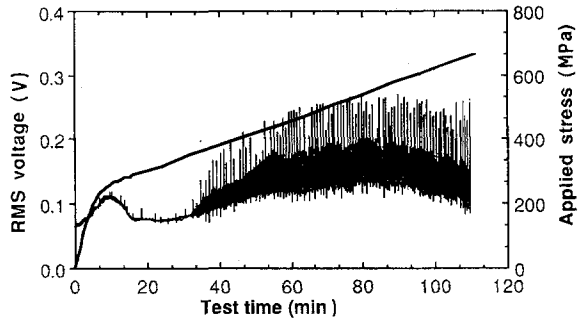

Figure 3 Copy of an actual data trace showing the load–deflection curve and the acoustic emission (shown in terms of the RMS voltage) generated from a sample from the 4L group. RMS voltage is shown as measured with no corrections, gain is 105 dB. Average nodule diameter is 0.088 mm.

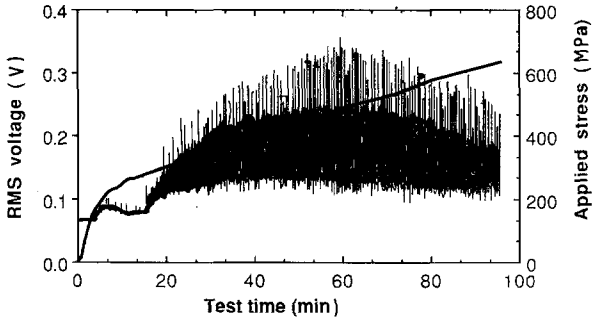

Figure 4 Copy of an actual data trace showing the load–deflection curve and the acoustic emission (shown in terms of the RMS voltage) generated from a sample from the 2U group. RMS voltage is shown as measured with no corrections, gain is 105 dB. Average nodule diameter is 0.123 mm.

agreement with theoretical predictions for the fracture of a brittle spherical particle in a plastic matrix [12, 13].

As mentioned earlier, Salzbrenner measured the fracture toughness of these materials according to ASTM E-813-81. The fracture toughness was found to be strongly dependent upon the size of the graphite nodules. Table III gives the values of the fracture toughness as determined by Salzbrenner and the average nodule diameter.

4. Discussion

The phenomenon of the acoustic emission generated by the fracture of an elastic spherical second-phase particle in a plastic matrix has been treated theoretically [12, 13] and has been the subject of a limited number of experimental investigations [9, 10, 11, 14]. The fundamental prediction of the present theory is that the magnitude of the acoustic emission generated by the fracture of the particle should depend on the diameter of the particle. A power-law dependence is predicted, i.e. the acoustic emission should be proportional to the particle diameter raised to some power. There is disagreement on the exact value of the power dependence, with values of 2 and 2.5 being predicted. The experimental data given in Table II can be plotted to determine the relationship between the measured acoustic emission and the particle diameter. Fig. 5 shows the magnitude of the second acoustic emission maxima from Table II plotted as a function of the average graphite nodule diameter on a log–log plot. A fair straight-line fit is obtained with a slope (or power dependence) of 0.96, which is considerably lower than predicted by any of the theoretical treatments. The lower power dependence is most likely due to additional acoustic emission in the second maximum caused by decohesion of the graphite nodules from the ferrite matrix.

Two recent publications have presented evidence that the decohesion between the particle and the matrix acts as a source of background or continuous emission and that the acoustic emissions generated by the actual fracture of the particles are the acoustic emission bursts above the background level [9, 13]. The data tabulated in Table II as "RMS 2nd maximum less back." is an attempt to evaluate the acoustic emission bursts at the second maximum with the background or continuous emission removed. These data are believed to be a result of the actual fracture of the graphite nodules. A log–log plot of "RMS 2nd maximum less back." data from Table II versus the

TABLE II

Sample no.	RMS 2nd maximum (μV)	RMS 2nd maximum less back. (μV)	Stress at second maximum (MPa)	Nodule diameter (mm)
5U	1.46 ± 0.09	1.03 ± 0.06	450 ± 20	0.136
2U	1.16 ± 0.07	0.76 ± 0.04	460 ± 20	0.123
1L	0.80 ± 0.04	0.36 ± 0.02	500 ± 20	0.078
4L	0.77 ± 0.04	0.40 ± 0.02	525 ± 25	0.088
7L	0.31 ± 0.02	0.04 ± 0.005	780 ± 30	0.031

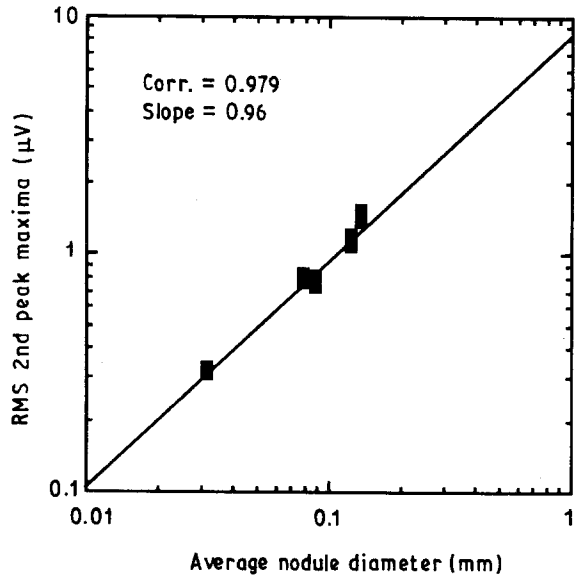

Figure 5 Log–log plot of the RMS second maximum versus the average nodule diameter.

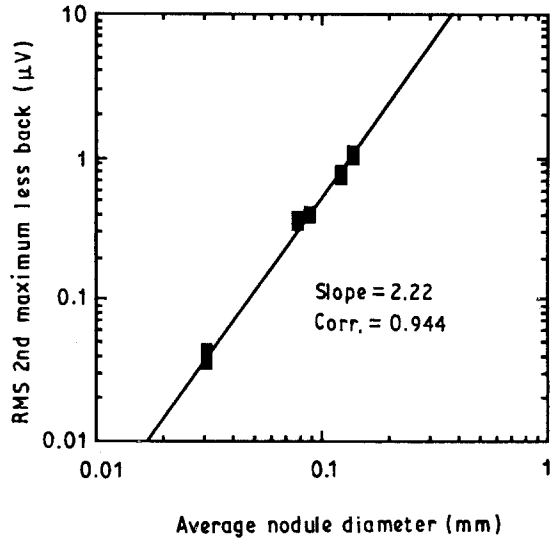

Figure 6 Log–log plot of the RMS 2nd maximum less background versus the average nodule diameter.

average nodule diameter is given in Fig. 6. A good straight-line fit is obtained with a slope (or power dependence) of 2.22, which is in excellent agreement with theoretical predictions. The excellent agreement with theoretical predictions provides strong evidence that the "RMS 2nd maximum less back." acoustic emission is generated by the fracture of the graphite nodules.

The strong dependence of the fracture toughness on the average nodule size (Table III) is not unexpected, and has been discussed in detail by Salzbrenner [5]. Fig. 7 gives a log–log plot of the fracture toughness as a function of the average nodule diameter. A straight line is obtained indicating a power-law dependence. The distance between nodules is essentially the ligament distance, or the average distance a crack will propagate before running into a barrier. A large nodule diameter for the same volume fraction of graphite means a larger ligament distance and, hence, a higher fracture toughness.

The purpose of the present study was to investigate any correlations between characteristics of the measured acoustic emission and the fracture toughness. To determine if correlations exist, it is necessary to compare the experimental acoustic emission data (Table II and Figs 5 and 6) with the fracture toughness of identical materials (Table III and Fig. 7). Plots of the acoustic emission data versus the fracture toughness are shown in Figs 8 (RMS 2nd maximum) and 9 (RMS 2nd maximum less background). In both cases a fairly good straight-line fit is obtained. There is little difference in correlation of the fracture toughness with either of the two RMS measurements and the correlation is good for the full range of measurements. From the data presented in Figs 8 and 9, a fairly accurate measure of the fracture toughness of ductile cast iron with low pearlite content could be obtained from analysis of the acoustic emission occurring after yield in a uniaxial compression test.

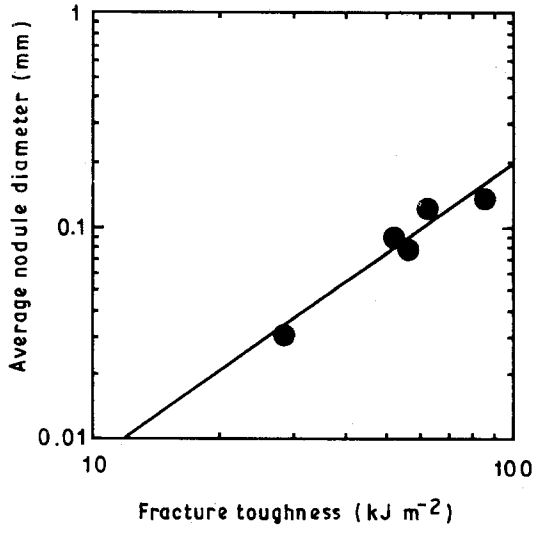

Figure 7 Log–log plot of the fracture toughness versus the average nodule diameter. Data are from Salzbrenner [5].

TABLE III Fracture toughness

Sample group number	Fracture toughness, J_{Ic} (kJ m^{-2})	Nodule diameter (mm)
5U	85.8	0.136
2U	62.7	0.123
1L	56.0	0.078
4L	51.7	0.088
7L	28.4	0.031

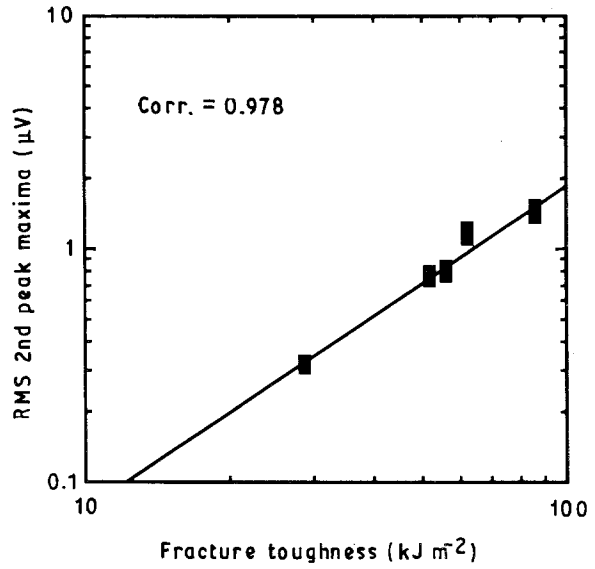

Figure 8 Log–log plot of the RMS second maximum versus the fracture toughness. Each data point is for samples with the same average nodule diameter.

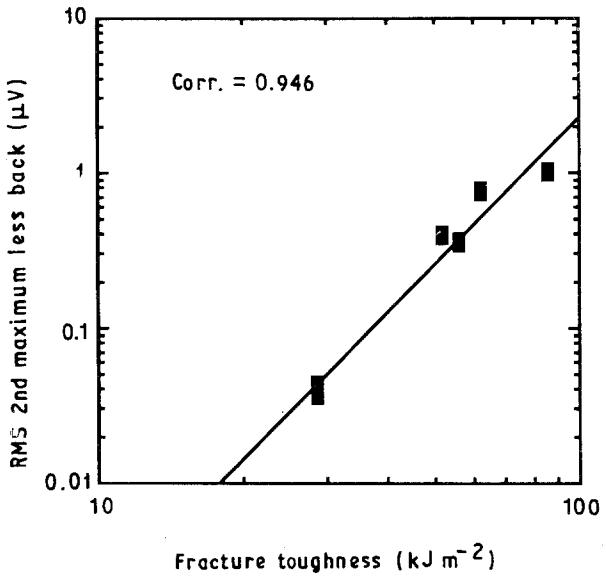

Figure 9 Log–log plot of the RMS 2nd maximum less background versus the fracture toughness. Each data point is for samples with the same average nodule diameter.

As mentioned earlier, the applied stress required to produce the fracture of a spherical particle is also dependent on the size of the particle. Gerberich and Jatavallabhula [13] have investigated the problem of the applied stress required to fracture a spherical elastic particle in a plastic matrix. They predict that the applied stress, σ, should be given by

$$\sigma = (1/q(e))(6E^*\gamma_c/d)^{1/2} \quad (1)$$

where $q(e)$ is a complicated strain concentration factor (which typically has a value slightly less than 2 and increases slowly with strain), γ_c is the specific work of fracture and E^* is the Young's modulus of the particle. Assuming that the location of the second acoustic emission maximum is a reasonable position measure the applied stress required to produce fracture of an average sized nodule, it is possible to investigate experimentally the validity of Equation 1. Fig. 10 is a log–log plot of the applied stress at the second maximum given in Table II versus the average nodule diameter. An excellent straight-line fit is obtained with a slope of 0.38, which agrees fairly well with the prediction of Equation 1.

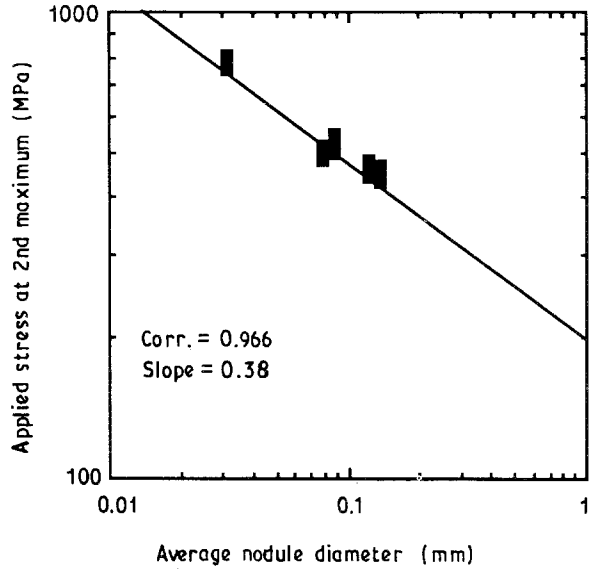

Figure 10 Log–log plot of the applied stress at the second RMS second maximum versus the average nodule diameter.

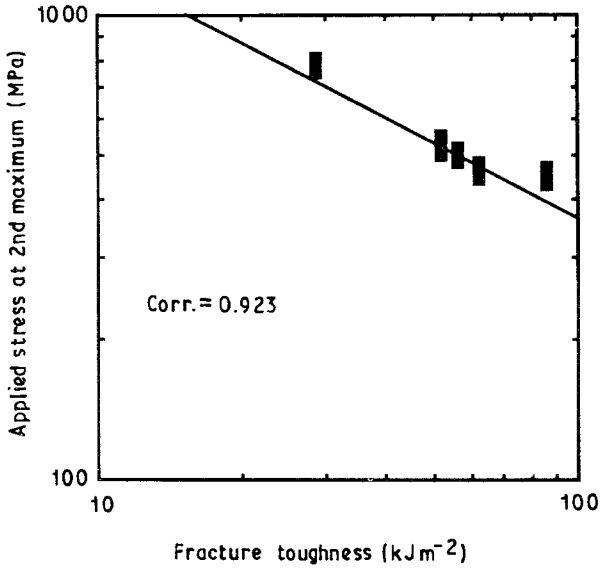

Figure 11 Log–log plot of the applied stress at the second RMS maximum versus the fracture toughness. Each data point is for samples with the same average nodule diameter.

Because both the applied stress required to cause fracture of a graphite nodule and the fracture toughness depend on the average nodule diameter, it is instructive to compare these two experimental quantities. Fig. 11 presents a plot of the applied stress measured at the second RMS maximum versus the fracture toughness for the same values of average nodule diameter. A good straight-line fit is obtained for the majority of the data; however, there are significant deviations at the larger nodules sizes which are responsible for high fracture toughness. It should be pointed out that even if an excellent correlation between applied stress and fracture toughness had been achieved, one could not simply obtain an estimate of the fracture toughness from the load–deflection curve. One would still need to carry out the acoustic emission measurements in order to identify the point in the load–deflection curve at which to evaluate the applied stress corresponding to the average nodule size, i.e. the 2nd RMS maximum.

5. Conclusions

The acoustic emission generated during the compressive deformation of nodular cast iron samples was measured and characterized. The sample material was identical to that used in a previous investigation to determine the fracture toughness [5]. Both the fracture toughness and certain features of the acoustic emission were found to be strongly dependent on the average diameter of the graphite nodules in the cast iron. The dependence of the acoustic emission from fracture and/or debonding of the graphite nodules was found to have a strong dependence on the nodule diameter. As suggested in the literature the acoustic emission from the actual fracture of the graphite nodules was obtained from subtracting the background or continuous emission from the burst-type emissions [9, 14]. The acoustic emission data treated in this fashion were in excellent agreement with theoretical predictions. A close correlation of the fracture toughness and the acoustic emission was obtained, indicating that it would be possible to determine the fracture toughness from acoustic emission measurements.

Data obtained also indicated that the stress required to fracture the graphite nodules can also be determined from the acoustic emission measurements and the load–deflection curve. The necessary stress for fracture was found to depend inversely on the nodule diameter as predicted by theory.

Acknowledgements

Portions of this work were supported by the United States Department of Energy through Grant DE-FG02-85ER45182. Their support is gratefully acknowledged. We thank Dr Richard Salzbrenner, Sandia National Laboratories, Albuquerque, NM, for providing the sample material.

References

1. "Ductile Iron", in "Metals Handbook", 9th Edn, Vol. 1, "Properties and Selection: Iron and Steels" (American Society for Metals, Metals Park, Ohio, 1978) pp. 33–56.
2. R. SALZBRENNER, J. A. VAN DEN AVYLE, T. J. LUTZ and W. L. BRADLEY, in "Proceedings, Sixteenth Symposium on Fracture Mechanics", ASTM STP 868, edited by M. F. Kanninen and A. T. Hopper (American Society for Testing and Materials, Philadelphia, 1985) pp. 328–44.
3. W. L. BRADLEY and H. E. MEAD Jr, in "Proceedings, American Foundry Society 84th Annual Meeting" (American Foundry Society, 1980) p. 126.
4. J. HWANG, J. DOONG and H. CHEN, *J. Mater. Sci. Lett.* **2** (1983) 737.
5. R. SALZBRENNER, *J. Mater. Sci.* **22** (1987) 2135.
6. T. F. DROUILLARD, "Acoustic Emission, A Bibliography with Abstracts" (IFI/Plenum, New York 1979).
7. S. H. CARPENTER and F. P. HIGGINS, in "Proceedings of the Third Acoustic Emission Symposium", edited by M. Onoe, Y. Ishii and T. Kameoka (Japan Industrial Planning Association, Tokyo, Japan, 1976) pp. 288–304.
8. D. M. EGLE, C. A. TATRO and A. E. BROWN, *Mater. Eval.* **39** (1981) 1037.
9. S. H.CARPENTER and Z. ZHU, *J. Acoust. Emiss.*, "Proceedings of World Meeting on Acoustic Emission, Charlotte, NC", 1989, Vol. 8, pp. 135–9 (extended abstract).
10. C. R. HEIPLE and S. H. CARPENTER, *J. Acoust. Emiss.* **6** (1987) 177.
11. *Idem., ibid.* **6** (1987) 215
12. R. KANT, Doctoral Thesis, University of California, Berkeley (1979).
13. W. W. GEBERICH and K. JATAVALLABHULA, in "Nondestructive Evaluation: Microstructural Characterization and Reliability Strategies", edited by O. Buck and S. M. Wolf (American Institute for Metallurgical Engineering, Warrendale, 1981).
14. C. R. HEIPLE and S. H. CARPENTER, *J. Acoust. Emiss.* "Proceedings of World Meeting on Acoustic Emission", Charollete, NC, 1989, Vol. 8, pp. 184–7 (extended abstract).

Received 28 September 1989
and accepted 9 April 1990